Applied Clay Science 112–113 (2015) 53–61

Contents lists available at ScienceDirect

Applied Clay Science

journal homepage: www.elsevier.com/locate/clay

Research paper

Technological properties of ceramic produced from steatite (soapstone) residues–kaolinite clay ceramic composites

Harlley Sander Silva Torres [a,*], Angélica Fortes Drummond Chicarino Varajão [b], Antônio Claret Soares Sabioni [c]

[a] IFMG-Campus Santa Luzia, Rua Érico Veríssimo, 370.B. Londrina, Santa Luzia, MG, 30115-190, Brazil
[b] Departamento de Geologia, Escola de Minas, Universidade Federal de Ouro Preto, Campus Universitário, Morro do Cruzeiro s/n, Ouro Preto, MG,35400-000, Brazil
[c] Departamento de Física, Universidade Federal de Ouro Preto, Campus Universitário, Morro do Cruzeiro s/n, Ouro Preto, MG, 35400-000, Brazil

ARTICLE INFO

Article history:
Received 22 April 2014
Received in revised form 13 April 2015
Accepted 18 April 2015
Available online 25 May 2015

Keywords:
Soapstone residues
Kaolinite clay
Composites

ABSTRACT

Ceramic bodies (7.0 cm × 2.0 cm × 1.0 cm) of kaolinite clay and soapstone residuals collected from workshops in Ouro Preto and Mariana, Minas Gerais, Brazil, containing from 2.5 to 97.5 wt% steatite (soapstone) were prepared and firing at 500, 1000 and 1200 °C, for 2 h, in air. The linear shrinkage, compressive strength, water absorption and mass loss by heating were determined on the samples after heat treatment. The fired samples at 1000 and 1200 °C, with steatite percentages of 85, 90 and 95%, presented the best results for technological applications in ceramic industry. For these samples, the values of the compressive strength were higher than 10 MPa and those of water absorption varied between 8 and 22%, which means that the values of these properties are superior and inferior, respectively, to the reference values established by Brazilian Standards. The linear shrinkage was lower than 6%, which is the maximum value established by the Pólo Cerâmico de Santa Gertrudes, in São Paulo State. These samples were chemically, mineralogically, and morphologically analyzed using ICP/OES, X-ray diffraction, Mössbauer spectroscopy, SEM and BET.

Talc and kaolinite were the dominant minerals, followed by quartz, chlorite, magnetite and magnesite. When firing at 1200 °C, the talc changes to enstatite and the appearance of mullite, periclase, hematite, clinoenstatite and protoenstatite occurs. The partial fusion of the talc promoted an increase in the liquid phase diminishing porosity and, consequently, water absorption. This process and the combination with mullite and periclase, increased the strength, reaching the values of 78 MPa, which is much greater than the minimum value of 10 MPa defined by the Brazilian Standard 15270-1 (ABNT 2005) for application on structural ceramic blocks.

1. Introduction

The southeastern region of Minas Gerais, Brazil, especially the Barroque cities of Ouro Preto and Mariana, is well-known for its soapstone art works that include traditional handicraft objects and kettles. This historical exploration of soapstone created handicraft shops, processing industries, separation and mass artifact production. These manipulation and production processes generate a great amount of fines that are normally discarded in inadequate places, being deposited in the soil and in waterways, causing silting and contamination. In addition, in this region, commonly occur kaolin deposits not yet industrially explored in spite of the great potential for the production of ceramics, paints, rubber, paper, pozzolanic material and mullite (Murray, 2007). The technological characterization of the kaolinite clay from this region has been the focus of various studies (Morales-Carrera et al., 2010; Peralta-Sánchez et al., 2011a,b) which showed the need for additional researches to enhance the kaolinite clay application in the ceramic industry. Talc, which is the principal mineral present in the steatite, has a trioctahedron structure of 2:1 layers with no charge on the layers. The layers are bonded by van der Waal forces (Sánchez-Soto et al., 1997; Wiewióra et al., 1997). This mineral has important properties for the manufacturing of many industrial products, such as cosmetics, pharmaceuticals, filler in paper, pesticides, polymers, paints, rubber and also in ceramics because of its low thermal and electrical conductivity and capacity to improve the mechanical characteristics and dimensional stability of ceramics (Sánchez-Soto et al., 1997; Dellisanti et al., 2009). During the heating of the mineral, water is liberated and amorphous phase and enstatite appear. The thermal treatments even give rise to other polymorphic forms such as protoenstatite and clinoenstatite (Wesolowski, 1984; Sánchez-Soto et al., 1997).

Therefore, the use of steatite residuals as additives to the ceramic mass can be an alternative to improve the quality of the kaolinite clay products besides contributing to the reduction of environmental pollution.

The principal objective of this study was to evaluate the properties of the ceramics produced from mixing kaolinite clay with the steatite (soapstone) residuals from the region of Ouro Preto and Mariana.

* Corresponding author. Instituto Federal de Minas Gerais. Rua Érico Veríssimo, 370. Bairro Londrina, Santa Luzia. MG. CEP 30115-190, Brazil.
E-mail addresses: harlley.torres@ifmg.edu.br (H.S.S. Torres), angelicavarajao@gmail.com (A.F.D.C. Varajão), claret.sabioni@gmail.com (A.C.S. Sabioni).

http://dx.doi.org/10.1016/j.clay.2015.04.016
0169-1317/

Table 1
Percentage (wt.%) of steatite (S) in the mixture steatite (S) + kaolinite clay (R5).

Sample	Mixture proportions	Sample	Mixture proportions	Sample	Mixture proportions
PR	R5	P5	R5 + S (20%)	P10	R5 + S (85%)
P1	R5 + S (2.5%)	P6	R5 + S (25%)	P11	R5 + S (90%)
P2	R5 + S (5%)	P7	R5 + S (50%)	P12	R5 + S (95%)
P3	R5 + S (10%)	P8	R5 + S (75%)	P13	R5 + S (97.5%)
P4	R5 + S (15%)	P9	R5 + S (80%)	PS	S

2. Materials and methods

Samples of steatite residuals (E) collected from handicraft shops in Cachoeira do Brumado, district of Mariana, and of kaolinite clay (R5) from a slope on highway BR-383, at 40 km from Ouro Preto, were dried at a temperature of 65 °C, for 72 h, in air, crushed and ground to yield a powder with a particle size suitable to pass through a #35 mesh (425 μm) sieve.

The humidity of steatite and kaolinite clay was measured in an electrical resistance ID200-Marte scale with 3 g of material for 3 min, followed by an adjustment of 10%; a value considered more adequate for the fabrication of the samples under pressure (Gaspar Júnior, 2003; Morales-Carrera et al., 2010). Fifteen samples were prepared containing different proportions of kaolinite clay and steatite (Table 1).

Bricks with a mass of 40 g and approximate dimensions of 7.0 cm × 2.0 cm × 1.0 cm, were molded at a velocity of 1 kN/s until reaching 50 kN, corresponding to a final pressure of 35 MPa, utilizing a uniaxial hydraulic press C1-SOLOCAP model LM-02, Digital Dynamometry Appea. Then, the bricks were dried in an oven at 65 °C, in air. Their dimensions were measured every 2 h until present dimensional stability. After this time, the bricks were kept in the oven for 24 h, totalizing 72 h. After drying, the bricks were fired at 500, 1000 and 1200 °C, for 2 h (plateau at the maximum temperature of treatment), in air, using the electric furnace Giron 1200. The heating rate was 5°/min. Through macroscopic analysis, without using equipment, samples were chosen that were free of systematic defects, such as cracks, chips, and surface irregularities. They also needed to be homogeneous in color and free of other or imperfections (ABNT, 1983). Other tests, such as linear firing shrinkage (LS), compressive strength (CS), bulk density (BD), water absorption (WA) and mass loss by heating (ML) at 1200 °C for 2 h were performed. For each sample, a total of three bricks per firing temperature were tested, and the average was recorded. Linear firing shrinkage (LS) of bricks was obtained from:

$$LS\,(\%) = (l1 - l2)\ 100 / l1.$$

where: l1 = length of bricks before firing and l2 = after firing.

Bulk density (BD) was calculated by the ratio of the mass (m) to volume (v):

$$BD = m/v$$

For WA test, the mass of bricks before firing was measured (M1). The bricks were soaked in boiling water for 2 h and cooled with running water. Then, the bricks were reweighed (M2). Water absorption capacity was determined as

$$WA = (M2 - M1) \times M1 \times 100$$

To determine ML, the mass of bricks before firing (M1) and after firing was weighed. Mass loss by heating was calculated as

$$ML = (M1 - M2) \times M1 \times 100$$

For these tests a Vernier caliper Mitutoyo and a precision balance Kern KB were used.

Mechanical tests NBR 15270-3 (ABNT, 2005) were executed using a uniaxial hydraulic press at a velocity of 1 kN/s, C1-SOLOCAP model LM-02, Digital Dynamometry Appea. Three samples, P10, P11 and P12, with the best results from the physical and technical tests were submitted to chemical, mineralogical and morphological analyses.

The chemical composition was determined by inductively coupled plasma/optical emission spectrometry (ICP/OES) with radial vision, Ciros CCD model, Spectro. The crystalline phases, before and after firing, were determined by X-ray diffraction (XRD) using a Panalytical EMPYREAN diffractometer with CuKα radiation, range of 2–70° 2θ, step size of 0.02 and counting time of 10 s. Morphological features were observed by scanning electron microscopy with X-ray microanalysis (SEM/EDS-Secondary Electrons), Vega 3 Tescam/Oxford, with gold coating. Volume fraction of porosity (pore volume) was measured by the nitrogen absorption using the Quantachrome BET (Brunauer-Emmett-Teller) model Nova 1200e. The N_2BET technique (Brunauer et al., 1938) is explained by the tendency of all solid surfaces of attracting molecules of surrounding gas, resulting in a process called gas sorption. The grain size distribution of the steatite and kaolinite clay was measured on a laser particle-measurement instrument, Cilas 1064, using the optical model Fraunhofer.

The Fe content and the type of Fe^{3+} and Fe^{2+} occupation in the raw and sintered phases were determined by Mössbauer spectroscopy (MS). Mössbauer spectra (MS) were collected at room temperature with a spectrometer using a constant-acceleration drive with triangular reference signal, 1024 channels (unfolded), and in the velocity range of −11 to +11 mm/s (increment of ~0.09 mm/s). The velocity was calibrated from the MS of a standard α-Fe foil at room temperature. The spectra were computer-fitted either with discrete Lorentzian sextets and/or doublets or with distributions of magnetic hyperfine fields.

3. Results

After drying at a temperature of 65 °C, for 72 h, the samples with the greatest quantity of R5 (Table 1), up to P7 (R5 + E(50%)), presented a reddish color (Fig. 1). This color turned to gray as the amounts of steatite content increased from P8 to PE. Laser particle size analysis for the kaolinite clay showed a mean particle size of 12.68 μm and a

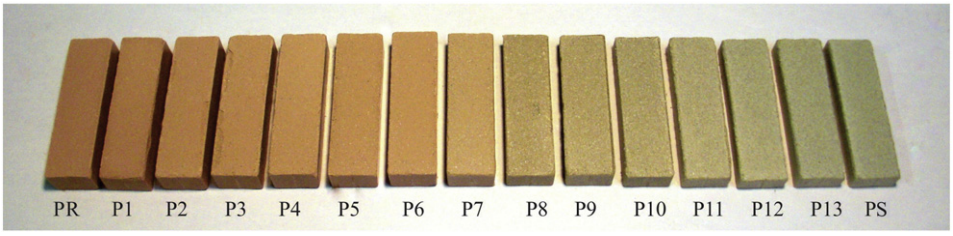

Fig. 1. Color evolution of the samples, evaluated macroscopically without instruments, after drying at a temperature of 65 °C, for 72 h, in air.

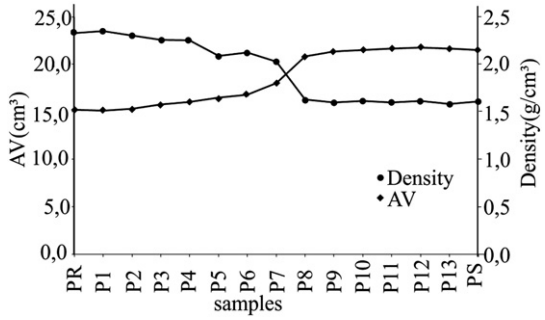

Fig. 2. Apparent volume (AV in cm^3) and bulk density (g/cm^3) in relationship to the amount of R5 in the composition of the green bodies after drying at 65 °C, for 72 h, in air.

predominant size of 20 μm. For steatite, the mean particle size was 22.68 μm and the predominant size was 27 μm.

The color turned from red to gray as the amount of steatite (soapstone) in the mixture was increased from P8 to PS (the compositions of the samples are given in Table 1).

The bricks with greater amount of R5 showed the apparent volume higher than those with greater S content, after drying at a temperature of 65 °C, for 72 h, in air (Fig. 2). The apparent volume of the bricks decreases as the amount of R5 content is reduced. This reduction is regular up to the P6 proportion. Between P6 and P8, the variation of the steatite content in the samples is greater (25%), directly reflecting in the apparent volume variation. From P8, the amount of steatite surpasses 75% and the apparent volume does not vary. From PR to P8, the bulk density increases from 1.52 to 2.15 g/cm^3 with the steatite increment (Fig. 2). The major difference occurs between P6 and P8 in function of the greater difference in the steatite quantity present in the samples (between 25% and 75%). From P8, the samples show a greater value for the bulk density: 2.15 g/cm^3.

The linear shrinkage for the bricks dried at 65 °C, for 72 h, in air, was less than 1%. The fired samples at 1000 and 1200 °C presented linear shrinkage (Fig. 3). The samples with greater amount of R5 (≥75% of kaolinite clay), such as P6, P5, P4, P3, P2, P1 and PR presented higher linear shrinkage with increasing temperature. For the steatite content greater or equal to 75%, the linear shrinkage varied little with the temperature and with the composition (LS ≤ 2%). The raw dried bricks with higher clay content showed greater apparent volume (Fig. 2). However, for the fired bricks with the same high clay content the effect is reversed, they show the highest percentage of linear shrinkage (Fig. 3(a)). The bricks fired at 500 °C showed a linear shrinkage of less than 1%.

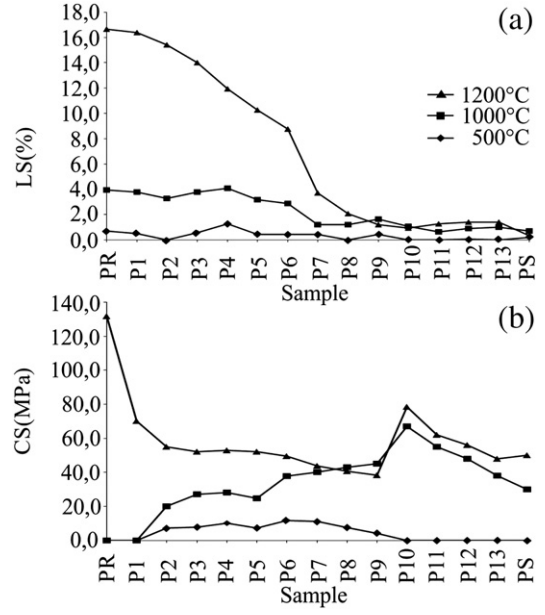

Fig. 3. (a) Linear shrinkage (LS) and (b) compressive strength (CS) of the fired samples in relationship with the amount of steatite present in the mixture, at three different temperatures.

Table 2
Chemical composition (ICP/OES) (wt.%) of the raw steatite (S), raw kaolinite clay (R5) and bricks fired at 1000 °C and 1200 °C.

T (°C)	Sample	SiO_2	Al_2O_3	Fe_2O_3	CaO	MgO	TiO_2	K_2O	MnO	LOI[a]
Natural	S	59.97	2.51	6.09	2.14	18.51	–	–	–	0.49
Natural	R5	43.14	34.69	5.37	0.05	0.04	2.02	0.54	0.17	0.5
1000	P8	50.8	14	9.18	3.05	22.9	0.72	0.16	0.11	0.49
	P9	49.9	12	9.09	3.03	23.9	0.62	0.13	0.11	0.81
	P10	49.8	10.1	9.64	3.46	25.5	0.5	0.1	0.11	0.7
	P11	49.8	8.54	9.84	3.45	26.8	0.42	0.07	0.12	0.61
	P12	49.5	6.88	10.4	3.73	28.1	0.32	0.04	0.13	0.67
	P13	49.6	5.98	10.6	3.83	29.1	0.27	0.03	0.13	0.79
1200	P8	49.8	13.5	9.05	2.91	22.3	0.7	0.18	0.1	0.1
	P9	50.6	12.1	9.68	3.26	24.2	0.61	0.14	0.12	0.03
	P10	50.6	10.5	9.79	3.41	26.2	0.51	0.1	0.12	0.08
	P11	49.2	8.54	9.91	3.49	26.6	0.41	0.07	0.12	0.1
	P12	50	6.97	10.4	3.72	28.4	0.32	0.05	0.13	0.08
	P13	50.4	6.02	10.8	3.92	29.4	0.27	0.03	0.14	0.11

[a] Mass loss on ignition.

For the compressive strength of the bricks fired at 1000 °C and at 1200 °C, except for PR and P1, the values are superior to the minimum values established by the Brazilian standard NBR15270-1 (ABNT, 2005), which vary between 1 MPa and 10 MPa, depending on the utilization of the ceramic bricks (Fig. 3(b)). However, taking into consideration the parameters visually observed by macroscopic analysis and the results of the linear shrinkage lower than 6% (reference value from the Pólo Cerâmico de Santa Gertrudes, in São Paulo State (Gaspar Júnior, 2003)), the samples selected were P8, P9, P10, P11, P12 and P13 fired at 1000 and 1200 °C. The chemical composition of these samples (Table 2) showed the predominance of SiO_2 and MgO, followed by Al_2O_3 e Fe_2O_3, with less amount of CaO. These samples were then submitted to analyses of water absorption and mass loss by heating tests.

The samples fired at 1200 °C have less water absorption than those fired at 1000 °C (Fig. 4), but the water absorption increases with the increase of steatite in the mixture.

The mass loss by heating is less when the mixture has greater quantities of steatite, but for all compositions, it increases around

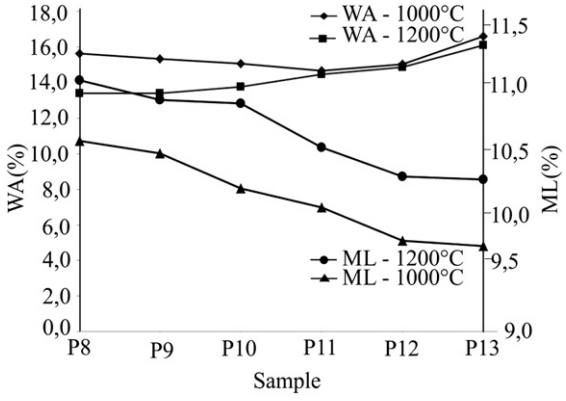

Fig. 4. Water absorption (WA) and mass loss by heating (ML) of the fired samples in relationship with the amount of steatite present in the mixture, at 1000 and 1200 °C for 2 h.

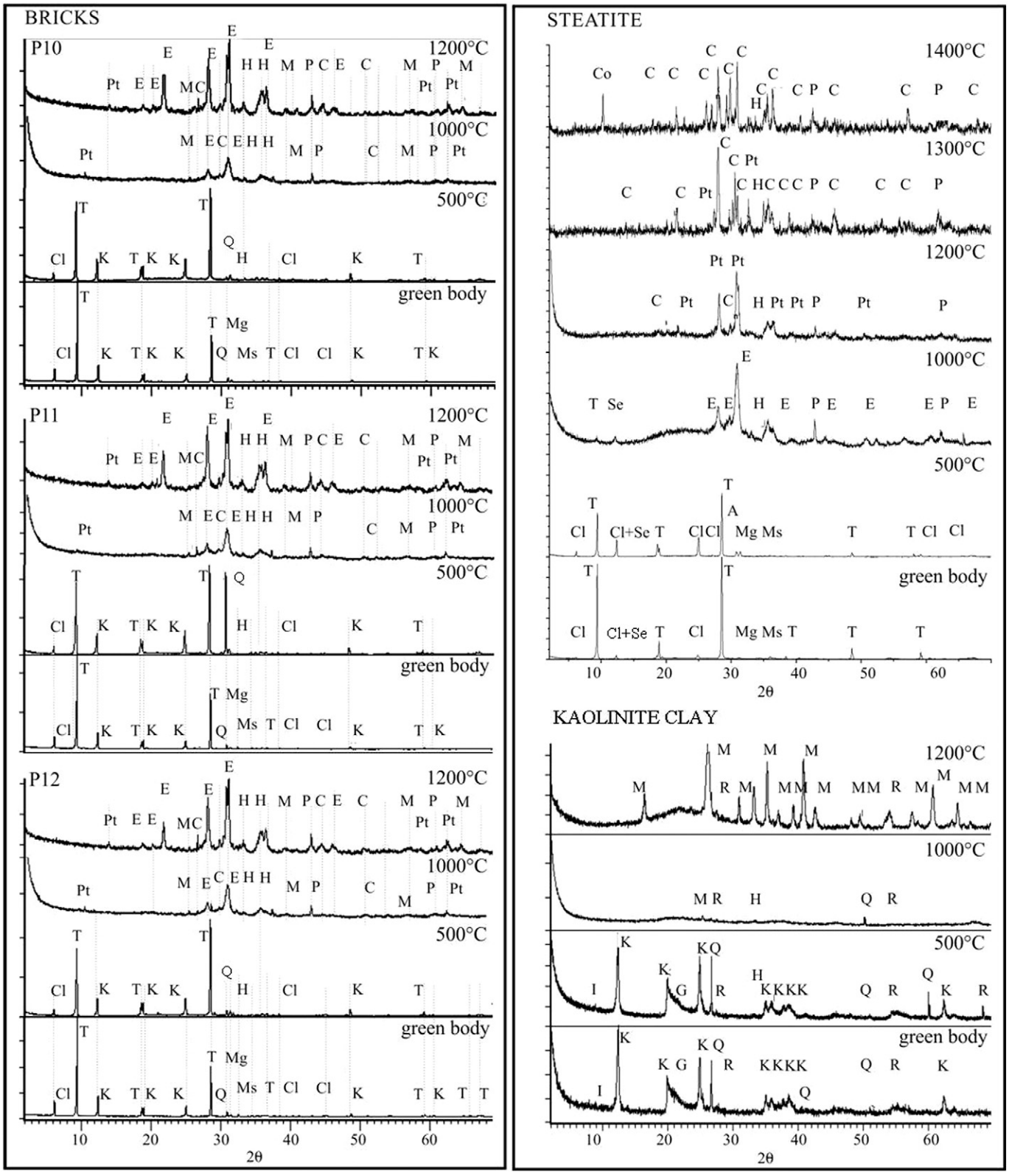

Fig. 5. X-ray patterns of sample steatite, kaolinite clay, P10, P11 and P12, raw and fired at 500, 1000 and 1200 °C. A: anatase; C: clinoenstatite; Cl: chlorite; Co: cordierite; E: enstatite; G: goethite, H: hematite; I: illite, K: kaolinite; M: mullite; Mg: magnetite; Ms: magnesite; P: periclase, Pt: protoenstatite; Q: quartz; R: rutile; Se: serpentine; T: talc.

0.5% when the heating temperature is increased from 1000 °C to 1200 °C (Fig. 4).

The P10, P11 and P12 samples showed the best results for the physical and technical tests and were thus, submitted to mineralogical and morphological analyses. The green bodies predominantly consisted of talc, kaolinite and chlorite, followed by quartz, magnesite and magnetite (Fig. 5(a), (b), (c)). At 500 °C, the mixtures still presented traces of talc, quartz, kaolinite and chlorite.

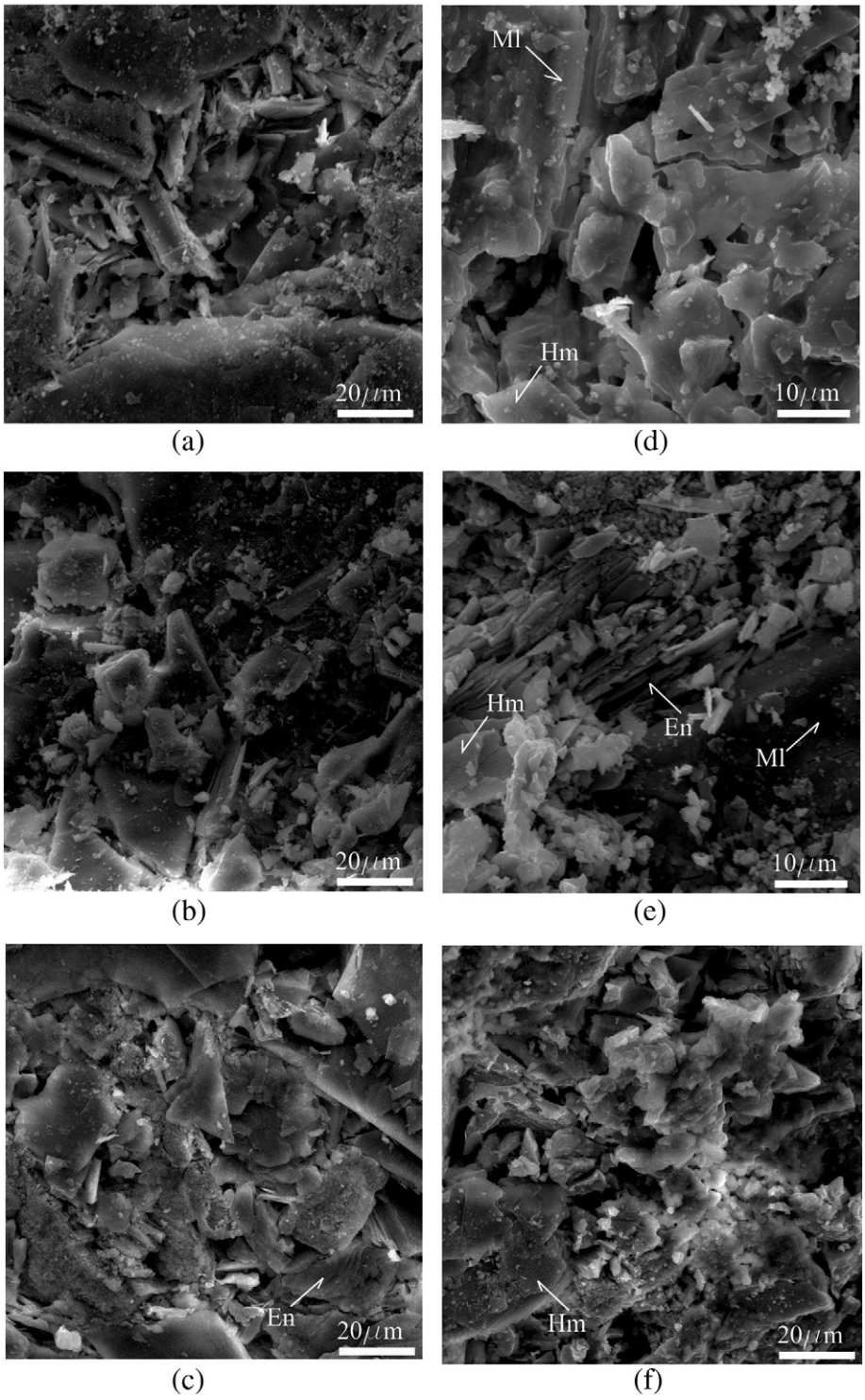

Fig. 6. Micrographies of samples P10 (a), P11 (b) and P12 (c) fired at 1000 °C and P10 (d), P11 (e) and P12 (f) fired at 1200 °C. En: enstatite, Hm: hematite, Ml: mullite.

At 1000 °C, the talc disappeared to give place to the enstatite ($Si_{16}Mg_{16}O_{48}$ JPDS 96-900-4118) and appeared hematite, periclase, small traces of clinoenstatite and an amorphous phase in P10 (Fig. 5(a)). At this temperature, there is formation of plate-shaped mullite grains with sizes ranging from 5 to 50 μm (Fig. 6(a), (b) and (c)). These same plates are covered with small grains which indicate the beginning of the sintering process in sample P11 (Fig. 7(b)).

At 1200 °C, the enstatite phase predominates, followed by hematite with traces of mullite, protoenstatite, clinoenstatite and periclase. At 1200 °C, it is possible to verify flaky structures typical of the enstatite phase resulting from talc transformation (Figs. 6(e) and 7(a)). The samples present large flakes and elongated forms with a high content of aluminum, characteristics of mullite, and deformed plaques of hematite (Fig. 6(d), (e) and (f)). The mullite appears more clearly as elongated grains in P10 (Fig. 6(d)) where there is the formation of necks, a characteristic that indicates the beginning of the sintering process, which is seen in regions where enstatite and hematite prevail (Fig. 7(a)). In all cases at 1000 °C, the surface was not compact, always having pores

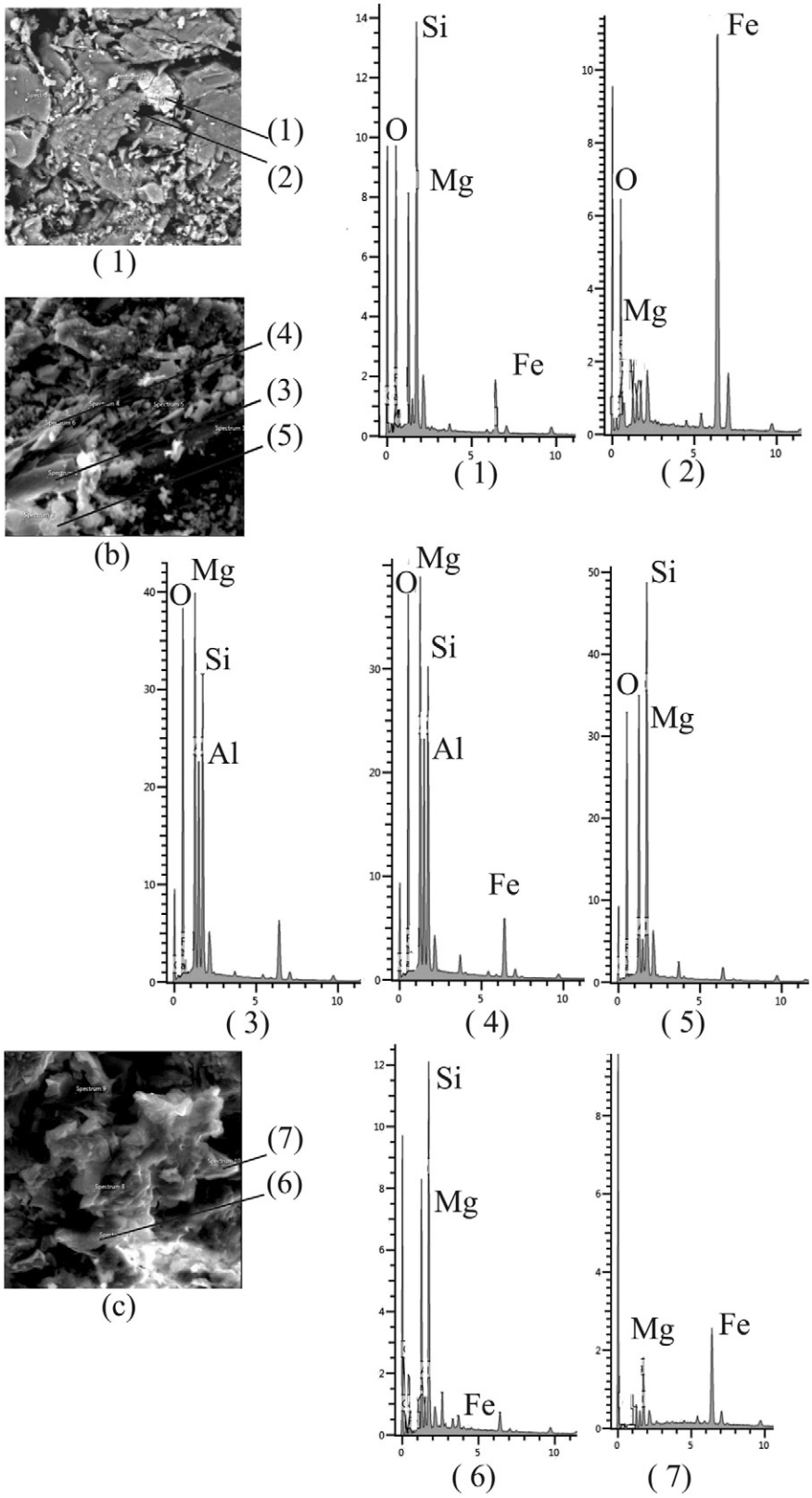

Fig. 7. EDS of the samples P10 (a), P11 (b) and P12 (c) firing at 1200 °C. Their analyses identified Mg, Si, Al and Fe in regions where there is the formation of (1, 5, 6 and 7) enstatite, (2) hematite and (3 and 4) mullite.

between the grains. The porosity diminished at 1200 °C in three of the samples. BET analysis confirmed this result, where P10 presented the lowest pore volume (Fig. 8).

The presence of Fe^{2+} and Fe^{3+} in samples P10, P11 and P12 was evaluated by means of Mössbauer spectra (Fig. 9), which showed similarities for the three samples. In their raw state, a small doublet indicates the

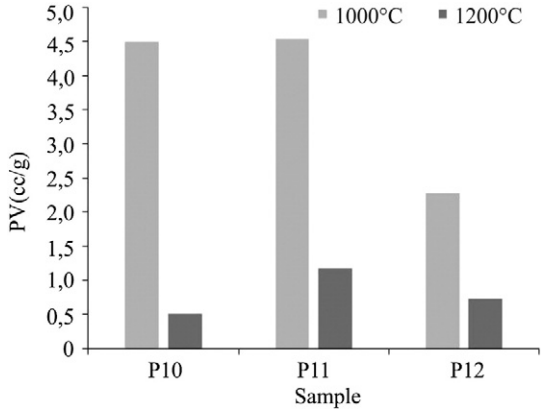

Fig. 8. BET analyses of pore volume (PV) of the samples fired at 1000 °C and 1200 °C.

presence of magnetite, while two doublets of Fe^{2+} and one of Fe^{3+} related to the hematite and chlorite. In the sample fired at 1000 °C, hematite appears and also a doublet of Fe^{3+} associated with the enstatite formation. At 1200 °C, besides the hematite and Fe^{3+}, the Fe^{2+} doublet appears, probably related to the enstatite.

4-. Discussion

The presence of R5 clay in the mixture inhibits the absorption of water (Fig. 4) and increases the linear shrinkage (Fig. 3) and the mass loss (Fig. 4). Therefore, samples P10, P11 and P12 present good results, especially those prepared at 1200 °C, because they conciliate lower mass loss with greater bulk density values, high compressive strength, and low values of linear firing shrinkage and water absorption.

According to Fig. 5 and Table 2, the chemical–mineralogical transformation of the talc due to heating is accompanied by a new arrangement in the tetrahedral layers of SiO_4. The formation of new phases passes through a structural reorganization when thermal decomposition occurs, modifying the physical properties of the ceramic bodies.

The formation of protoenstatite and amorphous silica at 1000 °C is a consequence of the dehydroxylation of talc at 850 °C and this process caused the weight loss (Wesolowski, 1984; Liu et al., 2014). The oxygen from the dehydroxylation creates a new arrangement in the amorphous phase which initiates the nucleation of the enstatite. Once the enstatite is formed, this new arrangement is predominant in the structure. Enstatite also predominates at 1200 °C. At 1000 °C, mullite begins to form, resulting from the sintering and crystallizing of the metakaolinite decomposition (Brasileiro et al., 2006; Magliano and Pandolfelli, 2010; Silva et al., 2011). The formation of the clinoenstatite is a consequence of the protoenstatite decomposition (Reynard et al., 2008) and from the enstatite, but its total crystallization only occurs at 1400 °C (Wesolowski, 1984). The protoenstatite to clinoenstatite and clino-to-proto inversions displayed the characteristics of martensitic transformation (Kelvin et al., 2010). This transformation is normally responsible to volume change (Vela et al., 2007; Reynard et al., 2008). Complete protoenstatite to clinoenstatite inversion would require rapid cooling (Mielcarek et al., 2004; Kelvin et al., 2010).

The magnesite decomposition generates periclase (Fig. 5) but the proportion of oxides was not modified with the thermal evolution from 1000 °C to 1200 °C, as shown in the ICP/OES analyses (Table 2).

The presence of magnetite is confirmed in the Mossbauer spectra (Fig. 8) that evolves into hematite at 1000 °C, in good agreement with the X-ray diffraction data. At this same temperature, and at 1200 °C, Fe^{2+} ions corroborate for the enstatite formation. In addition, the substitution of Mg^{2+} by Fe^{2+} can occur in the talc without unbalancing the charges (Gonçalves, 1991; Campos, 2001; Luz and Lins, 2005).

In sample P10, the presence of hematite is evident (Figs. 6(a), (d) and 7(a)) being responsible for the reddish coloring of the samples (Pérez et al., 2012). On the surface of the sample, the deformed flakes characterize the presence of enstatite at 1200 °C (Fig. 7(a)). The presence of periclase at 1000 °C accelerates mullite grain growth and diminishes the thermal expansion coefficient (Viswabaskaran et al., 2004; Kim et al., 2009).

Periclase contributes to sintering improvement and samples containing mullite displayed larger, more elongated grains with greater density, which consequently diminishes porosity and increases compressive strength (Viswabaskaran et al., 2004; Souto et al., 2009; Dong et al., 2011). The mullite is mainly seen at 1200 °C in the P10 and P11 samples (Figs. 6(d), (e), and 7(b)).

Where the talc content is greater (P12 > P11 > P10), the water absorption is also greater, due to the formation of pores caused by

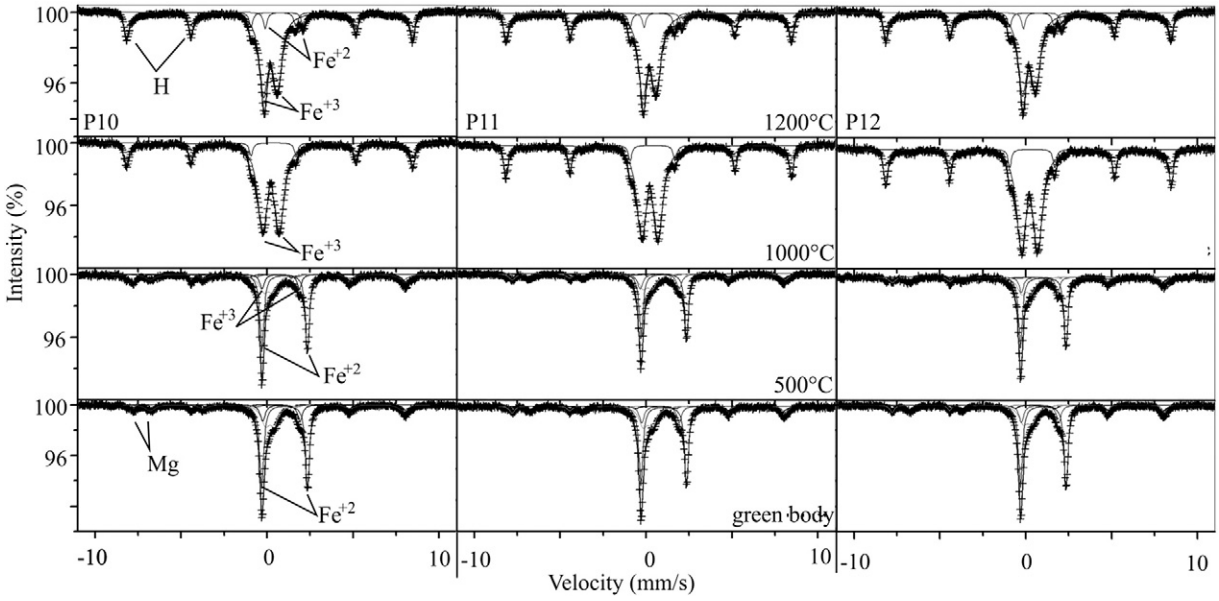

Fig. 9. Mössbauer spectra of samples P10, P11 and P12, raw (a) and fired at 500 (b), 1000 (c) and 1200 °C (d). Mg: magnetite, H: hematite.

water evaporation (Chandra et al., 2005). As the temperature increases from 1000 °C to 1200 °C, the partial fusion of the talc promotes an increase in the liquid phase which will progressively fill the pores, diminishing porosity and, consequently, water absorption. Water absorption is even lower for samples with the greatest amount of kaolinite clay at 1200 °C. There was a slight decrease of 2% in water absorption in P8 (Fig. 4) (Gökçe et al., 2011). By filling the pores, the liquid phase helps to densify the mass, generating a greater approximation of the particles, which results in a small retraction of the sintered ceramic piece (Souza and Holanda, 2005). Densification and sintering are slow processes in the function of the enstatite–protoenstatite transformation (Rohan et al., 2004; Gökçe et al., 2011). After firing at 1200 °C, P10 presented a lesser volume of pores (Fig. 8) and consequently, less water absorption was observed (Fig. 4) along with greater compressive strength (Fig. 3).

In spite of a small retraction, the centralization of the hydroxyl groups and the crystalline symmetry of the talc provided greater dimensional stability. To the contrary, kaolinite, that has hydroxyl groups on the surface, is thermally less stable and its presence provokes greater linear retraction (Wesolowski, 1984). Furthermore, heating kaolinite leads the formation of metakaolinite. The reaction kaolinite–metakaolinite generates vacancies in the lattice which are responsible for high sinterability of the material but they generate high linear shrinkage at temperatures higher (Magliano and Pandolfelli, 2010; Seynou et al., 2011).

Thus, the samples with the greatest amount of kaolinite clay (P10, for example), displayed greater linear shrinkage and lower water absorption.

Formation of mullite and the simultaneous decreasing of the porosity, at 1200 °C, favor the development of a microstructure that positively affects the mechanical properties, which consequently increased the sample densification during the firing process (Magliano and Pandolfelli, 2010; Ozel and Kurama, 2010). Likewise, the high compressive strength in P10 at 1200 °C is a consequence of the increase of enstatite and the appearance of protoenstatite, together with the formation of mullite, all these phases are associated with the mechanical properties of the material (Vela et al., 2007). The presence of protoenstatite, although in smaller quantities than enstatite, is critical to improve the mechanical strength. The protoenstatite is thermodynamically stable at high temperature because it is stabilized by the vitreous phase. Thus, it contributes for the sintering and to improve the mechanical strength. This change is characteristic of martensitic transformation (Mielcarek et al., 2004; Vela et al., 2007).

5. Conclusions

The physical, chemical, mineralogical and morphological characterization of the kaolinite clay/steatite ceramic samples demonstrated that a body containing 85% steatite (P10) presents adequate properties for possible technological applications. The compressive strength and linear firing shrinkage results were superior and inferior, respectively, to the values established by Brazilian standards. The presence of kaolinite clay in small amounts reduces water absorption. The transformation of kaolinite provoked sample linear shrinkage, but the presence of talc, the appearance of periclase and the growth of the mullite grains prevent this process. The partial fusion of the talc promoted an increase of the liquid phase resulting in decreased porosity and water absorption. As a consequence, there was an increase in sintering, density and compressive strength; in other words, the combination of sintering, mullite and periclase increased the compressive strength and the mechanical resistance.

Acknowledgments

The authors thank Fundação de Amparo à Pesquisa do Estado de Minas Gerais (FAPEMIG), Conselho Nacional de Desenvolvimento Científico e T.ecnológico (CNPq), CAPES, and the coordinators and staff of the Laboratories of the X-ray Diffraction of Geochemical (DEGEO), BET, Mossbauer Spectroscopy, SEM Laboratory – Redemat, and PROPP – Pró–Reitoria de Pesquisa e Pós-graduação – UFOP – Federal University of Ouro Preto. The authors also thank the editor and the two anonymous reviewers for their careful reading and suggestions to improve the manuscript.

References

ABNT - NBR 15270, 2005. Componentes cerâmicos. Parte 1: blocos cerâmicos para alvenaria de vedação—terminologia e requisitos, Rio de Janeiro (15 pp.).
ABNT- NBR 15270, 2005. Componentes cerâmicos. Parte 3: blocos cerâmicos para alvenaria estrutural e de vedação—métodos de ensaio, Rio de Janeiro (33 pp.
Brasileiro, M.L., Oliveira, D.H.S., Oliveira, M.F., Feves, G.A., Santana, L.N.L., 2006. Estudo da obtenção de mulita por meio de interações entre o resíduo de caulim e bay-clay sinterizados, e alumina em um processo termicamente ativado. 17° CBECIMat-Congresso Brasileiro de Engenharia e Ciência dos Materiais, Foz do Iguaçu, Brasil, 2006.
Brunauer, S., Emmett, P.H., Teller, E., 1938. Adsorption of gases in multi molecular layers. J. Am. Chem. Soc. 60, 309–319.
Campos, L.E.G., 2001. Talco e Pirofilita. Balanço Mineral Brasileiro. DNPM – Departamento Nacional de Produção Mineral, Ministério de Minas e Energia (19 pp.).
Chandra, N., Agnihotri, N., Bhasin, S., Khan, A.F., 2005. Effect of addition of talc on the sintering characteristics of fly ash based ceramic tiles. J. Eur. Ceram. Soc. 25, 81–88.
Dellisanti, F., Valdrè, G., Mondonico, M., 2009. Changes of the main physical and technological properties of talc due to mechanical strain. Appl. Clay Sci. 42, 398–404.
Dong, Y., Hampshire, S., Zhou, J.I.Z., Wang, J., Meng, G., 2011. Sintering and characterization of flyash-based mullite with MgO addition. J. Eur. Ceram. Soc. 31, 687–695.
Gaspar Júnior, L.A., 2003. Adição experimental de novos materiais às argilas da região do pólo cerâmico de Santa Gertrudes (SP). Tese, Departamento de Petrologia e Metalogenia. Universidade Estadual Paulista.
Gökçe, H., Agaogullari, D., LütfiÖvec, M., Duman, I., Boyraz, B., 2011. Characterization of microstructural and thermal properties of steatite/cordierite ceramics prepared by using natural raw material. J. Eur. Ceram. Soc. 31, 2741–2747.
Gonçalves, M.A., 1991. Estudo Mossbauer do esteatito (pedra-sabão). (Dissertação). Universidade Federal de Minas Gerais.
Kelvin, H., Ramesh, S., Tan, C.Y., Teng, W.D., 2010. Phase analysis and densification of steatite-based ceramics. Int. J. Automot. Mech. Eng. 1, 38–45.
Kim, B.M., Cho, Y.K., Stevens, R., Park, H.C., 2009. Mullite whiskers derived from kaolin. Ceram. Int. 35, 583–597.
Liu, X., Liu, X., Hu, Y.I., 2014. Investigation of the thermal decomposition of talc. Clay Clay Miner. 62, 137–144.
Luz, A.B., Lins, F.A., 2005. Rochas & minerais industriais: usos e especificações. CETEM/MCT, Rio de Janeiro (720 pp.).
Magliano, M.V.M., Pandolfelli, V.C., 2010. Binding systems for mulitizied castables. Cerâmica 56, 112–117.
Mielcarek, W., Nowak-Wozny, D., Prociów, K., 2004. Correlation between $MgSiO_3$ phases and mechanical durability of steatite ceramics. J. Eur. Ceram. Soc. 24, 3817–3821.
Morales-Carrera, A.M., Peralta-Sánchez, M.G., Varajão, A.F.D.C., Ferreira, M.M., 2010. Aproveitamento de argilas cauliníticas naturais e com aditivos do Quadrilátero Ferrífero na obtenção de materiais cerâmicos. Técnicas Aplicadas a la Caracterización y Aprovechamiento de Recursos Geológico-Mineiros vol. 1. CYTED e IGME, Madrid.
Murray, H.H., 2007. Applied Clay Mineralogy: Occurrences, Processing and Applications of Caulins, Bentonites, Palygorskite-Seppiolite, and Common Clays. Developments in Clay Science. 2 (180 pp.).
Ozel, E., Kurama, S., 2010. Effect of the processing on the production of cordierite-mullite composite. Ceram. Int. 36, 1033–1039.
Peralta-Sánchez, M.G., Morales-Carrera, A.M., Varajao, A.F.D.C., 2011a. Modificação de superfícies cerâmicas através de ativação alcalina. In: Alvarado, E.B., Dominguez, M.J. (Eds.), Técnicas Aplicadas a la Caracterización y Aprovechamiento de Recursos Geológico-Mineiros - Procesos experimentales" vol. 2. CYTED e IGME, Oviedo.
Peralta-Sánchez, M.G., Morales-Carrera, A.M., Varajão, A.F.D.C., Ferreira, M.M., 2011b. Viabilidade do uso de argilas cauliníticas do Quadrilátero Ferrífero para a indústria cerâmica. Cerâmica 57, 254–262.
Pérez, J.M., Rincón, J.Mª., Romero, M., 2012. Effect of moulding pressure on microstructure and technological properties of porcelain stoneware. Ceram. Int. 38, 317–325.
Reynard, B., Bass, J.D., Jackson, J.M., 2008. Rapid identification of steatite–enstatite polymorphs at various temperatures. J. Eur. Ceram. Soc. 28, 2459–2462.
Rohan, P., Neufuss, K., Matejícek, J., Dubský, J.L., Prchlík, L., Holzgartner, C., 2004. Thermal and mechanical properties of cordierite, mullite and steatite produced by plasma spraying. Ceram. Int. 30, 597–603.
Sánchez-Soto, P.J., Wiewióra, A., Avilés, M.A., Justo, A., Pérez-Maqueda, L.A., Pérez-Rodríguez, J.L., Bylina, P., 1997. Talc from Puebla de Lillo, Spain. II. Effect of dry griding on particle size and shape. Appl. Clay Sci. 12, 297–312.
Seynou, M., Millogo, Y., Ouedraogo, R., Traoré, K., Tirlock, J., 2011. Firing transformation and properties of tiles a clay from Burkina. Appl. Clay Sci. 51, 499–502.
Silva, R.A., Teixeira, S.R., Souza, A.E., Santos, D.I., Romero, M., Rincón, J.Mª., 2011. Nucleation kinetics of crystalline phases from a kaolinitic body used in the processing of red ceramics. Appl. Clay Sci. 52, 165–170.
Souto, P.M., Menezes, R.R., Kiminami, R.H.G.A., 2009. Sintering of commercial mullite powder: effect of MgO dopant. J. Mater. Process. Technol. 209, 548–553.

Souza, S.J.G., Holanda, J.N.F., 2005. Avaliação das propriedades físico-mecânicas de uma massa cerâmica para revestimento poroso (BIII). Cerâmica 51, 70–76.
Vela, E., Peiteado, M., Garcia, F., Caballero, A.C., Fernández, 2007. Sintering behaviour of steatite materials with barium carbonate flux. Ceram. Int. 33, 1325–1329.
Viswabaskaran, V., Gnanam, F.D., Balasubramanian, M., 2004. Mullite from clay-reactive alumina for insulating substrate application. Appl. Clay Sci. 25, 29–35.
Wesolowski, M., 1984. Thermal decomposition of talc: a review. Thermochim. Acta 78, 395–421.
Wiewióra, A., Sánchez-Soto, P.J., Avilés, M.A., Justo, A., Pérez-Maqueda, L.A., Pérez-Rodríguez, J.L., Bylina, P., 1997. Talc from Puebla de Lillo, Spain. I. XRD study. Appl. Clay Sci. 12, 233–245.